Design for Cascade of Crossflow Direct Contact Membrane Distillation

Jack Gilron,*,† Liming Song, and Kamalesh K. Sirkar*

Otto H. York Department of Chemical Engineering, New Jersey Institute of Technology, Newark, New Jersey 07102

The use of crossflow direct contact membrane distillation (XF-DCMD) modules allows lower velocities and volumetric flows on the brine side while still maintaining good heat-transfer coefficients. The key to using these modules in energy-efficient processes requires that the heat be recovered from the hot distillate exit stream with close temperatures of approach. This is best accomplished in a cascade of crossflow modules arranged in a manner approaching the behavior of countercurrent DCMD modules. A short-cut design method is presented to determine the number of such identical modules needed to extract maximum heat recovery between an inlet and exit brine temperature. This method is dependent on two observations: (1) existence of a unique relationship between brine temperature drop across a stage (ΔT_{stage}) and the temperature of closest approach between brine and distillate streams at the top of the stage (ΔT_{end}), which defines an operating line; (2) ΔT_{end} remains relatively constant from stage to stage. As in other thermal processes, there is a tradeoff between energy efficiency and area (here, membrane area). The optimum will be a function of the relative costs of energy and membrane area. For brine entrance and exit temperatures of 95 °C and 32−38 °C, respectively, and a specific stage area of 2.9 m^2/(mt/h), the optimum number of stages moves from six to two as the price of energy decreases from $4 US/mt steam equivalent to $0.73 US/mt steam equivalent.

1. Introduction

Much work has been performed in the last 20 years in regard to exploring the use of direct contact membrane distillation (DCMD) processes for desalination and process stream treatment for the concentration of materials. This work has been surveyed in detail in several recent comprehensive reviews.[1−3] In a DCMD process, hot brine flows at atmospheric pressure on one side of a porous hydrophobic membrane and cold distillate flows on the other side of the membrane. Water vapor that has been evaporated from the hot brine at the brine/membrane pore interface diffuses through the pores and is condensed at the pore/distillate interface on the other side of the membrane at a lower temperature. This thermal technique is inherently superior to reverse osmosis-based processes for concentrate management, because the water vapor flux reduction is minor as the salt concentration is increased from, for example, 0.5% to 10%.[1] Using the correlations[1] of water vapor pressure with temperature and salt concentration, only a 0.8 °C temperature increase is needed to compensate the water vapor pressure drop, because of the brine concentration increase from 0.5% to 10% in the feed. Therefore, such thermal techniques are ideal for the following goals: (1) very high water recovery from brackish/seawater feeds; (2) managing the concentrate from desalination processes, including reverse osmosis (RO); and (3) desalination in inland areas and recovering water from industrial brines.

The typical mode of operation with such DCMD modules is in countercurrent operation with heat recovery. This is illustrated in Figure 1. This has been done in hollow fiber modules with an external heat exchanger for heat recovery[4] and also in an integrated spiral wound unit in which the heat recovery occurs within the spiral by placing a cold feed channel next to the condensing distillate channel separated by a metal foil wall.[5]

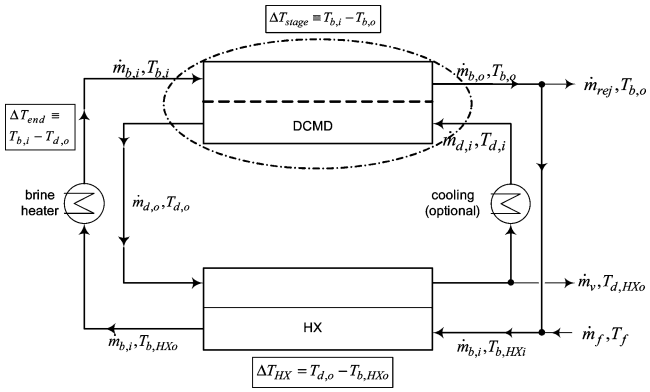

Figure 1. Schematic of a countercurrent direct contact membrane distillation (DCMD) module with a heat recovery heat exchanger and equal mass flows on the brine and distillate sides.

In these DCMD modules, which are operated in countercurrent fashion, the inlet mass flow rates are approximately equal and, thus, the temperature difference between brine and distillate streams is maintained at a constant value throughout the membrane module fixed by the desired temperature of closest approach, where y is an arbitrary distance along the brine flow path:

$$T_{\text{b}}(y) - T_{\text{d}}(y) = \Delta T_{\text{end}} \equiv T_{\text{b,i}} - T_{\text{d,o}} \tag{1}$$

As has been shown by others,[2,4] the specific energy input for such a countercurrent arrangement will be

$$\frac{Q_{\text{in}}}{\dot{m}_V} = \frac{C_P \dot{m}_{\text{b,i}}(T_{\text{b,i}} - T_{\text{b,HXo}})}{\dot{m}_V} = \frac{C_P(\Delta T_{\text{end}} + \Delta T_{\text{HX}})}{R} \tag{2}$$

where, by heat balance, the recovery per DCMD module is

* To whom correspondence should be addressed. For J.G.: Tel.: +972-8-6461921. Fax: +972-8-6472960. E-mail address: jgilron@bgu.ac.il. For K.K.S.: Tel.: 973-596-8447. Fax: 973-642-4854. E-mail address: sirkar@adm.njit.edu.

† On leave from Ben-Gurion University, Beer Sheva, Israel 84105.

10.1021/ie060999k CCC: $37.00
Published on Web 03/16/2007

$$R \equiv \frac{\dot{m}_V}{\dot{m}_{b,i}} = \frac{\eta C_P (T_{b,i} - T_{b,o})}{\Delta H_V - C_P(\eta T_{b,o} - \langle T_{b,m} \rangle)} = \frac{\eta C_P \Delta T_{stage}}{\Delta H_V - C_P(\eta T_{b,o} - \langle T_{b,m} \rangle)} \quad (3)$$

where ΔT_{stage} is the temperature drop in the brine stream as it passes through the DCMD module, $\langle T_{b,m} \rangle$ the average temperature of the brine at the membrane surface weighted by vapor flux at each temperature, and η the thermal efficiency (vapor-mediated enthalpy transfer rate divided by the total heat-transfer rate). If one uses typical brine inlet and exit temperatures of 90 and 40 °C, respectively, giving a ΔT_{stage} value of ~50 °C, and average thermal efficiencies reported in the literature of ~60%,[4,6] one finds that recoveries cannot exceed more than 7% in a single pass. To this end, one must use partial brine recycle, as illustrated in Figure 1, or a series of such countercurrent DCMD modules. It can be shown that the analysis for one pass of the brine through the DCMD module will be valid, regardless of whether part of the brine is recycled. When brine recycle exists, the analysis for heat recovery is conducted as if the heat exchanger and DCMD were operating in an once-through mode with the feed temperature at the heat recovery heat exchanger inlet being the same as the temperature of the brine exiting the DCMD module. This is illustrated in Figure 2. As shown in the schematic in the lower half of Figure 2, the makeup feed with a mass flow rate of $\dot{m}_f$ is heated up to the brine recycle temperature ($T_{b,o}$) by the warmer distillate stream in a heat exchanger (HX2). As shown in the left portion of the temperature−enthalpy diagram in the upper part of Figure 2, the makeup mass flow rate is much smaller (higher slope of the cold stream temperature−enthalpy curve) than the distillate stream, and so it heats up much more than the distillate stream cools. At the entrance to heat exchanger HX1, the warmed makeup feed is mixed with the recycled brine, which has a mass flow rate of $\dot{m}_{b,o} - \dot{m}_{b,rej}$, where $\dot{m}_{b,rej}$ is the mass flow rate of the rejected brine stream. As shown in the right portion of the temperature enthalpy diagram in the upper part of Figure 2, the mass flow rate of the combined stream of the makeup and recycle is the same as $\dot{m}_{b,i}$, which is the same as the warm distillate stream from which heat is then recovered in HX1.

Assuming we have a relationship of $\Delta H_V - C_P(\eta T_{b,o} - \langle T_{b,m} \rangle) \approx \Delta H_V$, then the specific energy input is given by[4]

$$\frac{Q_{in}}{\dot{m}_V} \approx \left(\frac{\Delta T_{end} + \Delta T_{HX}}{\eta \Delta T_{stage}} \right) \Delta H_V \quad (4)$$

From eqs 1 and 4, we see that the DCMD module is constrained to operate at a temperature difference of closest approach ($\Delta T_{end} = T_{b,i} - T_{d,o}$), which is dictated by the desired specific energy consumption for a given terminal temperature difference of the heat exchanger. In addition, the effort to minimize temperature polarization leads to running the brine in the lumen side, which generates significant pressure drops on the brine side.[4] Although developed for countercurrent DCMD modules, the aforementioned results are also relevant to a crossflow contact pattern arranged in a cascade, as shown below.

Li and Sirkar[6] have recently developed a highly efficient hollow fiber crossflow module for the DCMD process, in which the water vapor fluxes obtained were very high and the temperature polarization was minimized with relatively low Reynolds numbers ($Re = 58-68$). For similar brine mass flow rates, the crossflow module had much less temperature polarization than a parallel flow module, such as that which would be used in true countercurrent operation. The crossflow module could be operated as a stand-alone module; however, in this case, the energy efficiencies are very low. Preliminary calculations (see below) show that the highest gained output ratio (GOR) for equal mass flows of distillate and brine would be no better than 2.2. Therefore, a design approach was sought to combine such crossflow modules into a countercurrent cascade that would combine the energy efficiencies of true countercurrent DCMD with the advantages of crossflow modules.

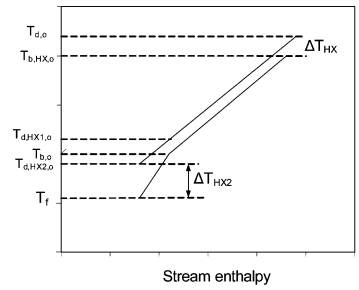

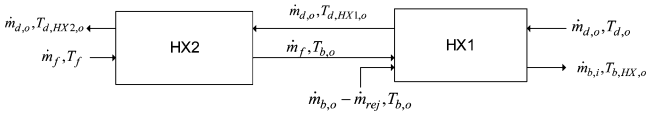

Figure 2. Arrangement of heat exchangers for heat recovery in DCMD with partial brine recycle.

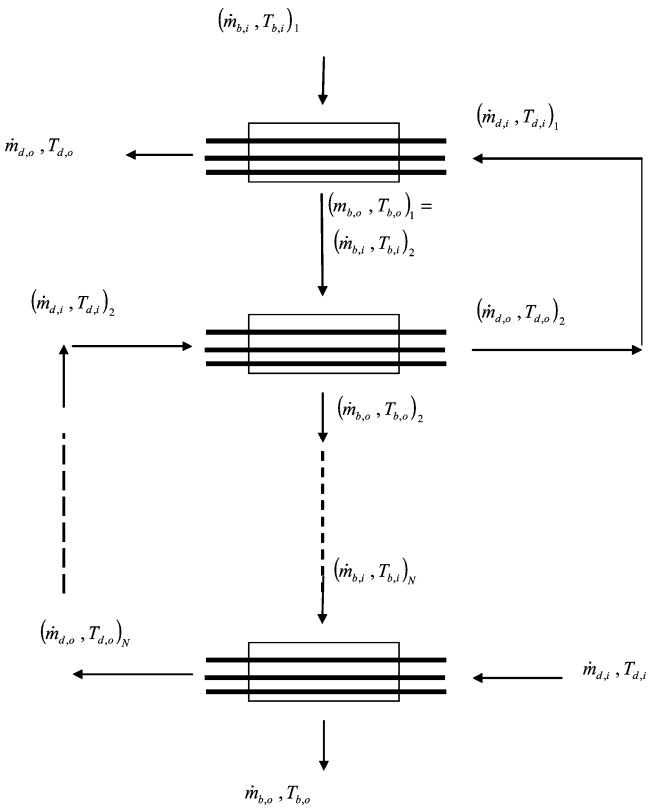

Figure 3. Scheme for using crossflow DCMD modules to obtain a countercurrent cascade.

2. Development of Design Equations

2.1. Stage Matching Requirements. If we combine several crossflow units together in a countercurrent design, it will have the format illustrated in Figure 3. In this case, the countercurrent cascade of crossflow DCMD modules would represent the single DCMD block shown in Figure 1. A heat balance taken around

an individual stage provides the following relation:

$$(T_{d,o} - T_{d,i}) = \frac{\dot{m}_{b,o}}{\dot{m}_{d,i}}(T_{b,i} - T_{b,o}) + \frac{\dot{m}_V}{\dot{m}_{d,i}}(T_{b,i} - T_{d,o}) \quad (5)$$

which relates the extent of temperature increase in the distillate stream to the temperature decrease in the brine stream. Because of the fact that the required heat input of the brine heater decreases with lower ΔT_{end}, the last term should be as small as possible. In the case where $m_{b,i} = m_{d,o}$, as described previously, then $m_{b,o} = m_{d,i}$ and

$$T_{d,o} - T_{d,i} = (T_{b,i} - T_{b,o}) + \frac{\dot{m}_V}{\dot{m}_{d,i}}(T_{b,i} - T_{d,o})$$

which can be rearranged to give

$$T_{b,o} - T_{d,i} = (T_{b,i} - T_{d,o}) + \frac{\dot{m}_V}{\dot{m}_{d,i}}(T_{b,i} - T_{d,o}) = \left(1 + \frac{\dot{m}_V}{\dot{m}_{d,i}}\right)(T_{b,i} - T_{d,o}) \quad (6)$$

If several DCMD modules are placed in series, with respect to their brine and distillate flows, then the brine outlet and distillate inlet of one stage will be the brine inlet and distillate outlet of the next stage (see Figure 3):

$$(T_{b,o} - T_{d,i})_j = (T_{b,i} - T_{d,o})_{j+1} \quad (7)$$

Substituting this relation into the previous equation and using the definition of $(\Delta T_{end})_j = (T_{b,i})_j - (T_{d,o})_j$, analogous to eq 1, to denote the closest approach temperature for the jth stage of a series of DCMD modules, we have

$$(\Delta T_{end})_{j+1} = \left(1 + \frac{\dot{m}_V}{\dot{m}_{d,i}}\right)_j (\Delta T_{end})_j \quad (8)$$

This shows that, to match the streams of subsequent stages in the DCMD, the closest temperature difference at each subsequent DCMD stage can only increase by a factor of $(\dot{m}_V/\dot{m}_{d,i})_j$, which is usually $\ll$1%. Therefore, the temperature of closest approach is defined by the top temperature of closest approach. The cost of having a larger temperature difference on stages that are further downstream to increase flux is the requirement to apply interstage heating.

2.2. Crossflow DCMD Module Simulator. To use this analysis to design a countercurrent cascade of crossflow modules, we must have a crossflow DCMD module simulator. This simulator must predict the relationship between the decrease in the stage brine temperature and the temperature of closest approach for each stage, as a function of brine inlet temperature. In another publication, we present this module simulator, which was successful in reasonably predicting the experimental performance for laboratory-scale and bench-scale crossflow DCMD modules.[7] Here, we only present the assumptions and basic equations used in the simulator. These are as follows:

(1) The brine and distillate streams enter at uniform temperatures.

(2) No mixing of the brine stream occurs along the fiber axis (this is a reasonable assumption considering that brine velocity is much higher than any sideways mixing).

(3) The heat capacity was taken to be constant over the temperature ranges shown.

(4) All other fluid properties were obtained from functions developed from tables of properties of pure water.[8]

(5) The brine vapor pressure was assumed to be equal to that of pure water. This is a reasonable assumption for these modules, as shown by experiments with up to 10% of simple salt solutions.[7]

(6) The membrane vapor permeance, as defined in eq 11, was assumed to be an empirical constant. This has been used by other investigators, regardless of whether the permeance is via a mechanism of Knudsen diffusion, Knudsen−viscous transition flow, or a combined Knudsen−molecular diffusion mechanism.[1,3]

The solution film heat-transfer equations for the brine and distillate sides are given by

$$\frac{1}{\alpha}\left(\frac{dQ(x)}{dx}\right)_j = h_p A_{rp}(T_{pm}(x) - T_p(x))_j \quad \text{(tube side)} \quad (9a)$$

$$\frac{1}{\alpha}\left(\frac{dQ(x)}{dx}\right)_j = h_f A_{rf}(T_f(x) - T_{fm}(x))_j \quad \text{(shell side)} \quad (9b)$$

where

$$A_{rf} = \frac{d_o}{d_i}$$

$$A_{rp} = \frac{d_i}{d_i} = 1$$

and

$$\alpha = n_j \pi d_i$$

where the left-hand side of each equation is the total heat flux, with respect to the lumen-side membrane surface area of the jth layer and n_j refers to the number of fibers in the jth layer. In our case, we will use an equal number of fibers in each layer, although a more general module could be used with varying numbers of fibers in each layer. It can be shown that, for the heat fluxes concerned, eqs 9 represent a good approximation of the exponential temperature polarization profiles found in this type of module.

The total heat flux is given by contributions from both conduction and mass-transfer mediated enthalpy convection, which can be defined at the fiber−lumen boundary:[9]

$$\frac{1}{\alpha}\left(\frac{dQ(x)}{dx}\right)_j = h_m A_{rln}(T_{fm}(x) - T_{pm}(x)) + N_v(x) A_{rln} H(T_{pm}) = h_m A_{rln}(T_{fm}(x) - T_{pm}(x)) + N_v(x) A_{rln}(\Delta H_V(T_{pm}) + C_P T_{pm}) \quad (10)$$

where

$$A_{rln} = \frac{d_{lm}}{d_i}$$

where C_P refers to the heat capacity of liquid water.

The distillate flux, with respect to the logarithmic mean area, is given by

$$N_v(x) = k_m(p_{fm}(x) - p_{pm}(x)) \quad (11)$$

where k_m is the effective vapor permeance. The value used here was $A_{rln}k_m = 0.0024$ kg/(m^2 h Pa), which provides a good match

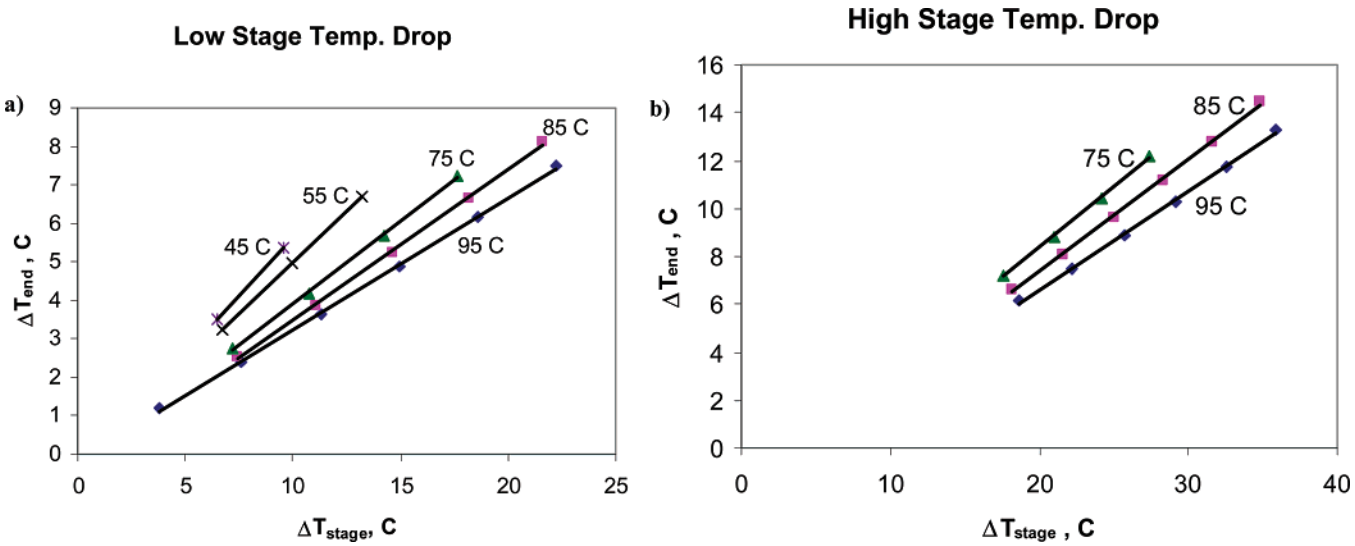

Figure 4. Dependence of the temperature of closest approach on the decrease in brine temperature through the stage, for 2.9 m^2/(mt/h): (a) low decreases in stage temperature (<20 °C) and (b) high decreases in stage temperature (>20 °C).

Table 1. Linear Coefficients Relating the Decrease in Stage Temperature (ΔT_{stage}) to the DCMD Temperature of Closest Approach (ΔT_{end}) When ΔT_{stage} < 20 °C, for Various Specific Stage Areas

	$\Delta T_{end} = a_1 \Delta T_{stage} + a_0$					
	1.9 m^2/(mt/h) (52 layers)		2.9 m^2/(mt/h) (78 layers)		5.8 m^2/(mt/h) (156 layers)	
$T_{b,i}$ (°C)	a_1	a_0	a_1	a_0	a_1	a_0
45	0.804	−0.409	0.590	−0.307	0.369	−0.194
55	0.728	−0.542	0.538	−0.407	0.340	−0.258
75	0.587	−0.705	0.430	−0.402	0.279	−0.259
85	0.529	−0.721	0.391	−0.419	0.257	−0.272
95	0.448	−0.273	0.343	−0.199	0.237	−0.260

to the experimental bench-scale data.[7] The vapor pressures are given by the Antoine equation:

$$p_{fm}(x) = \exp\left(23.1964 - \frac{3816.44}{T_{fm}(x) + 273.15 - 46.13}\right) \quad (12)$$

The heat-transfer coefficients used in eqs 9 are given by the Zukauskas equation[10] on the shell side and by the asymptotic value of the Nusselt number (4.36) on the tube side. Previous work on crossflow vacuum membrane distillation[11] showed the appropriateness of the Zukauskas equation for the shell-side heat transfer, whereas Zarkadas and Sirkar showed that the asymptotic Nusselt number is a better correlation of tube-side heat transfer than is the Seider−Tate method in a hollow fiber polymeric heat exchanger.[12] This is also supported by simulations by Gryta and Tomaszewska.[9]

The overall heat-transfer coefficient for the membrane is given by

$$h_m = \epsilon h_{mg} + (1 - \epsilon) h_{ms} \quad (13)$$

which is an area-averaged heat-transfer coefficient for pores (h_{mg}) and the membrane matrix (h_{ms}), where ϵ is the membrane porosity.

The mass balance for the jth layer of the module along the distillate path and along the brine path is given by the following equations:

$$\int_0^L [N_v(x)]_j A_{rln} \alpha \, dx = (\dot{m}_p(L) - \dot{m}_p(0))_j = (\dot{m}_f)_{j-1} - (\dot{m}_f)_j \quad (14)$$

The heat balance for the jth layer of the module along the distillate and brine path is given by the following equations:

$$[Q(x_1)]_j = \int_0^{x_1} d[Q(x)]_j = C_p[\dot{m}_d(x_1)T_d(x_1) - \dot{m}_d(0)T_d(0)]_j = \frac{C_p}{L}\int_0^{x_1} [(\dot{m}_f(x)T_f(x))_{j-1} - (\dot{m}_f(x)T_f(x))_j] \, dx \quad (15)$$

where the term $[\dot{m}_f(x)]_j$ refers to the brine mass flow rate leaving layer j if all the brine flow had a value corresponding to position x along the fibers in layer j.

The set of eqs 9−15 is implicit for the variables T_{fm}, T_{pm}, and T_p and can be solved through a nonlinear solver, by assuming a given constant value for the vapor permeance (k_m). This was programmed in Matlab, and results were generated for differing inlet conditions of brine and distillate flow rates and temperatures ($\dot{m}_{b,i}$, $T_{b,i}$, $\dot{m}_{d,i}$, and $T_{d,i}$). The inlet brine and distillate flow rates were set so that the brine inlet flow rates and distillate outlet flow rates were equal ($\dot{m}_{b,i} = \dot{m}_{d,o}$), so that enthalpy matching would be observed in the heat recovery heat exchanger.

2.3. Simulation Results−Correlations of Operating Variables, $T_{b,i}$, ΔT_{stage}, and ΔT_{end}. The crossflow DCMD simulator was operated for a series of brine and distillate inlet temperatures for several families of DCMD modules, with each family having a different number of layers that were multiples of 26 (52, 78, 156) for a constant mass flow rate. The simulated module had 100 fibers per layer, with the same brine entrance window dimensions (25.5 cm × 8.6 cm) as the larger experimental unit, described elsewhere.[7,13] This corresponded to a specific stage area ($\bar{a}$) that ranged from 1.9 m^2/(mt/h) to 5.8 m^2/(mt/h) of brine inlet flow rate, based on the internal lumen area. Using

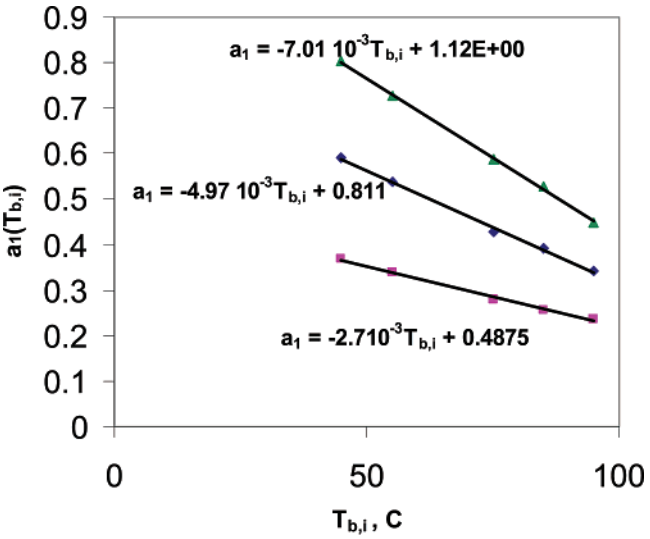

Figure 5. Dependence of the linear temperature coefficient on the brine inlet temperature. Specific stage areas for each curves are (▲) 1.9 m^2/(mt/h), (◆) 2.9 m^2/(mt/h), and (■) 5.8 m^2/(mt/h).

this method, a series of curves were generated that connected the decrease in stage temperature (ΔT_{stage}) to the temperature of closest approach for the DCMD stage (ΔT_{end}). A typical result is provided in Figure 4a. Because the dependence changes at very high ΔT_{stage} (>20 °C), a separate linear correlation was developed in this range (see Figure 4b). As can be seen, there is a linear relationship between ΔT_{end} and ΔT_{stage} for each brine inlet temperature and specific stage area:

$$\Delta T_{end} = a_1 \Delta T_{stage} + a_0 \tag{16}$$

A listing of the linear coefficients found at each temperature is provided in Table 1. From this table, a linear correlation can be generated for the linear coefficients (a_1) and the brine inlet temperature for moderate decreases in stage temperature. This is shown in Figure 5 for specific stage areas ranging from 1.9 m^2/mt/h to 5.8 m^2/mt/h for brine inlet temperatures of 45−95 °C. For greater decreases in stage temperature, the dependence of the linear coefficients a_1 and a_0 with the brine inlet temperature ($T_{b,i}$) are quadratic, as shown in Figure 6 for a specific stage area of 2.9 m^2/(mt/h). Table 1 and Figure 5 show that, as the specific stage area increases, ΔT_{end} decreases for a given ΔT_{stage} (as shown by the linear coefficients). This means that, for a given recovery per stage, a greater specific stage area allows for lower energy consumption, as shown in eq 4. Also, from the point of view of distillate pressure decrease per stage, it is preferred to have the largest number of layers, because then the cross section for distillate flow increases in linear proportion with the number of layers (specific stage area). For the module geometry simulated, the pressure decrease for 2.9 m^2/(mt/h) is 0.14 bar, not counting entrance and exit effects. If the specific stage area is too small, then the maximum number of stages in a cascade may be limited by the high distillate pressure decrease per stage.

In contrast, the lumen-side area-based flux per stage significantly decreased as the specific stage area increased (see Figure 7). This is because, with greater specific stage area, the linear velocity of the distillate stream is lower, which leads to vanishingly small temperature differences earlier along the length of the distillate flow path. As a result, less of the total membrane area is well-exploited.

As shown in Table 1, for moderate decreases in stage temperature, the intercepts are very small (<0.5 °C) and have a tendency to be fairly constant. They can be set equal to a constant average value for the different brine inlet temperatures, because the intercept uncertainty is well within the overall uncertainty of the simulator predictions. For larger decreases in stage temperature (>20 °C), the intercept a_0 is described by a quadratic equation (Figure 6), which can be used for interpolation in cascade design. This will only be required at high inlet temperatures, where large decreases in stage temperature are likely.

Similarly, the thermal efficiency for a particular stage is given by a multiple linear equation that is strongly dependent on the inlet brine temperature to the stage ($T_{b,i}$) and is weakly dependent on the decrease in brine temperature of the stage (ΔT_{stage}). For two different specific stage areas, we get

$$\eta\ (2.9\ m^2/(mt/h)) = 0.21 + 7.45 \times 10^{-3} T_{b,i} - 3.88 \times 10^{-3} \Delta T_{stage} \quad (R^2 = 0.977) \tag{17a}$$

$$\eta\ (5.8\ m^2/(mt/h)) = 0.212 + 7.42 \times 10^{-3} T_{b,i} - 3.67 \times 10^{-3} \Delta T_{stage} \quad (R^2 = 0.977) \tag{17b}$$

As can be seen, the thermal efficiency is almost independent of the specific stage area used. Using these correlations and eqs 17, one can rewrite the equation for the specific energy input for a single crossflow module, in terms of the decrease of stage temperature for a given inlet temperature ($T_{b,i}$):

$$\frac{Q_{in}}{\dot{m}_V} \approx \left(\frac{a_1(T_{b,i}, \Delta T_{stage}) \Delta T_{stage} + a_0 + \Delta T_{HX}}{\eta(T_{b,i}) \Delta T_{stage}} \right) \Delta H_V \tag{18}$$

or, in terms of the gained output ratio (GOR)-mt distillate/mt steam equivalent heat,

$$GOR \approx \frac{\eta(T_{b,i}, \Delta T_{stage}) \Delta T_{stage}}{(a_1(T_{b,i}) \Delta T_{stage} + a_0 + \Delta T_{HX})} \tag{19}$$

When this is done for a crossflow module operated with 5.8 m^2/mt/h and 2 °C temperature of approach in the heat exchanger (ΔT_{HX}), one finds there is an optimal decrease in stage temperature, as illustrated in Figure 8. This could be expected, given that the decrease in stage temperature appears in both the denominator and numerator of eq 19.

3. Cascade Design Methodology

Now, using the simulator curves, we can generate a cascade of crossflow stages (usually of identical construction and area), starting at a given brine inlet temperature and targeting a given brine outlet temperature with a defined temperature of closest approach. This is illustrated in Figure 9 for a specific stage area of 2.9 m^2/(mt/h). In this example, the temperature difference of closest approach in each DCMD stage is 4 °C, as shown by the horizontal dotted line. The brine inlet is at 95 °C. The slanted lines represent the operating lines appropriate for the brine inlet temperature of each stage. The operating line is given by rewriting eq 16, in terms of the stage exit temperature $T_{b,o}$ to give

$$\Delta T_{end} = a_1(T_{b,i} - T_{b,o}) + a_0$$

where the coefficients a_1 and a_0 are functions of the stage brine inlet temperature, as described previously. By following the ΔT_{end} vs $T_{b,o}$ operating line that is appropriate for 95 °C, we observe its intersection with the line of constant ΔT_{end} and read

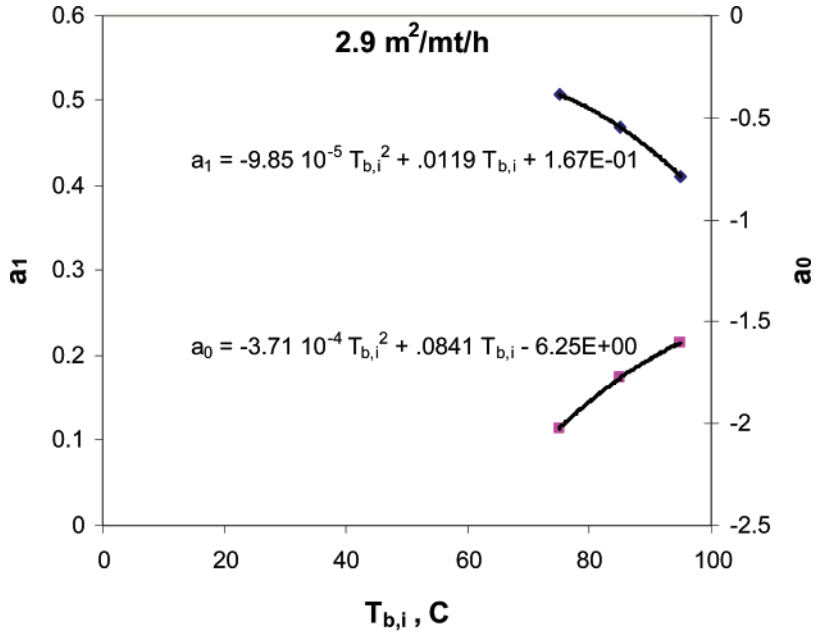

Figure 6. Dependence of the linear coefficients in eq 16 on the inlet brine temperature to the crossflow stage with high decreases in stage temperature (ΔT_{stage} > 20 °C).

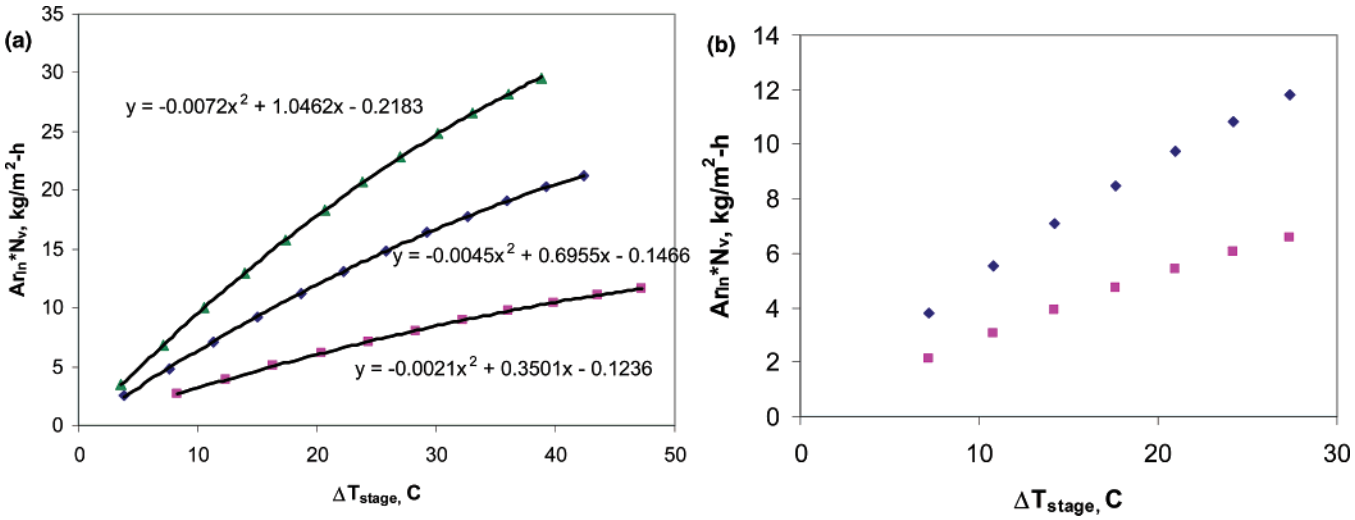

Figure 7. Dependence of lumen-side area-based flux on the decrease in stage brine temperature for different specific stage areas: (a) $T_{b,i}$ = 95 °C and (b) $T_{b,i}$ = 75 °C. Legend: (▲) 1.9 m²/(mt/h), (◆) 2.9 m²/(mt/h), and (■) 5.8 m²/(mt/h).

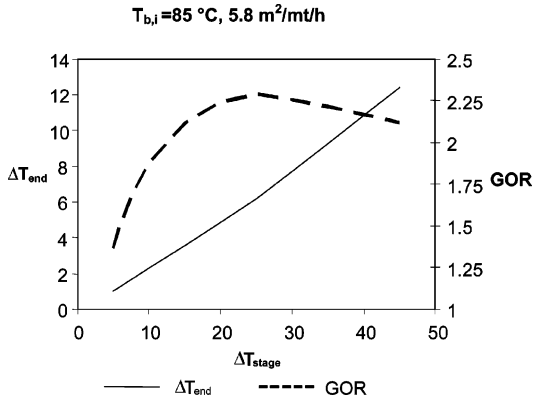

Figure 8. Single-stage crossflow DCMD, as a function of the decrease in stage brine temperature. Note that optimum operation from point of view of gained output ratio (GOR) is $\Delta T_{stage} \approx 23-24$ °C.

off the brine outlet temperature $T_{b,o}$ from the first stage from the *x*-axis (see the right-most vertical dotted line in Figure 9). Now, we again follow the operating line appropriate for the $T_{b,o}$ value from the first stage, which is the $T_{b,i}$ value for the second stage, and repeat the procedure. In such a way, we can step off the number of stages to get to a certain minimum brine exit temperature from the cascade, similar to generating stages in a McCabe−Thiele diagram.

Using a computer version of this approach coded in MATLAB, a series of cascades were generated for different temperatures of closest approach. The results are shown in Figures 10 and 11. In Figure 10, we show the brine outlet and distillate inlet temperatures at the bottom of the cascade, for varying numbers of stages in series. Their difference represents the temperature of closest approach, as expected from eq 7. Assuming a heat exchanger temperature difference (ΔT_{HX}) of 2 °C, we can then generate the GOR for each cascade by rewriting eq 4 for the brine temperature decrease through the entire cascade, instead of through an individual stage:

$$\mathrm{GOR} \equiv \frac{\Delta H_v}{Q_{in}/\dot{m}_v} = \eta\left(\frac{\Delta T_{cascade}}{\Delta T_{end} + \Delta T_{HX}}\right) \qquad (20)$$

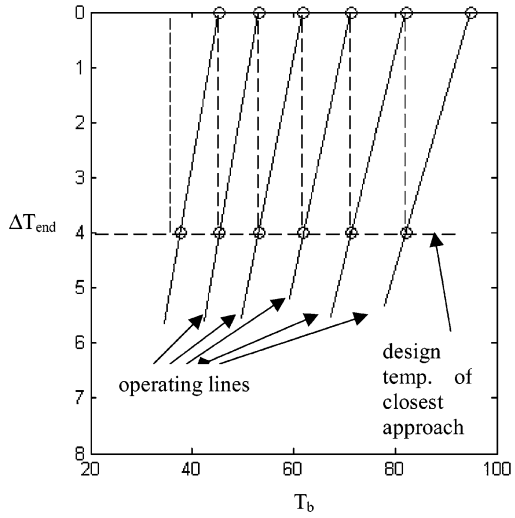

Figure 9. Determination of the number of stages required to take brine from 95 °C to ~32 °C with $\Delta T_{end} = 4$ °C and a specific stage area of 2.9 m^2/(mt/h).

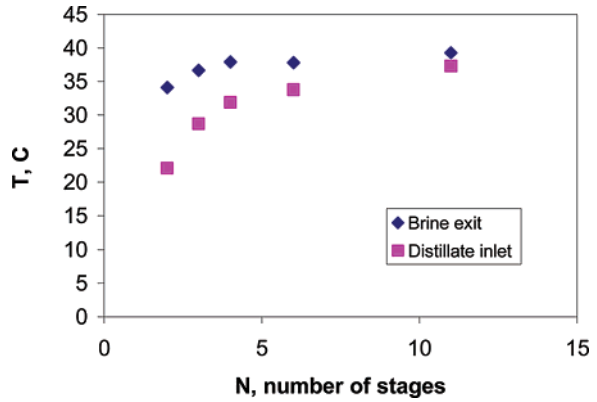

Figure 10. Different DCMD cascades for different temperatures of closest approach (ΔT_{end}), with $T_{b,i} = 95$ °C and $\bar{a} = 2.9$ m^2/(mt/h).

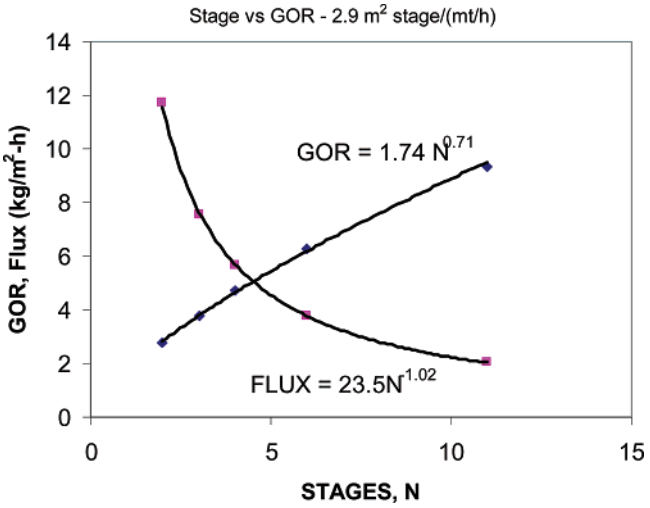

Figure 11. Tradeoff between GOR, flux, and the number of stages in cascades, with $T_{b,i} = 95$ °C.

Given an upper temperature of 95 °C, a bottom brine temperature of 35 °C, and an efficiency of 70%, and assuming that only 2 °C is the temperature of closest approach on the DCMD module and 1 °C is the temperature of closest approach on the HX module, the GOR would be ~14. If one only took a temperature difference slightly greater than that required to overcome vapor pressure depression for a 10% solution and allowed the temperature difference in the heat exchanger to be only 1 °C, then one could increase the GOR to ~21.

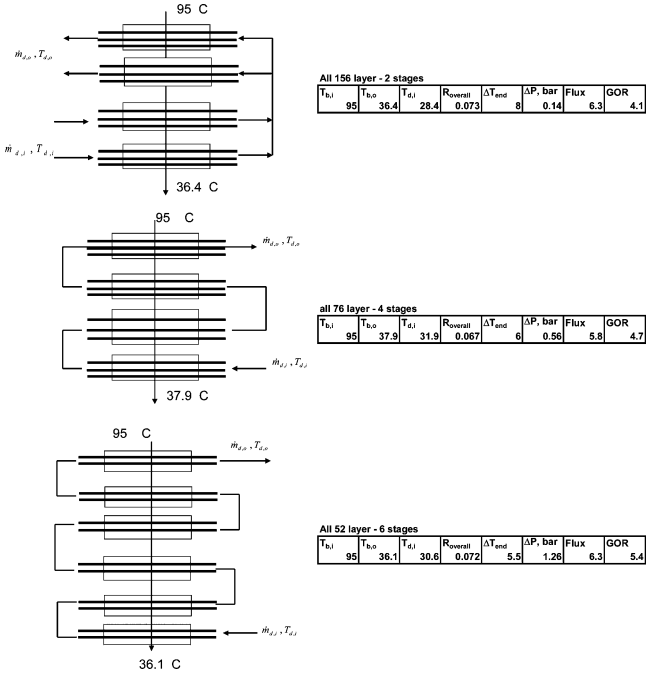

Figure 12. DCMD cascades with equal total membrane area with $T_{b,i} = 95$ °C. The tradeoff between the number of internal stages and GOR also is shown.

From eq 20, the results in Figure 11 are generated, which shows the tradeoff between GOR, flux, and the number of stages. As more stages N are used, the GOR improves significantly. Clearly, there will be an optimum (see section 4).

To determine the effect of internal staging on the distillate flow, we compared the results for three cascades with the same total amount of membrane area: six modules with 52 layers ($\bar{a} = 1.9$ m^2/(mt/h))), four modules with 78 layers per module ($\bar{a} = 2.9$ m^2/(mt/h)), and two modules of 156 layers per module ($\bar{a} = 5.8$ m^2/(mt/h)) operating over approximately the same range of brine inlet and outlet temperatures from the cascade. These results are shown in Figure 12. It can be seen that the fluxes are approximately equal, although the initial brine-distillate temperature difference for each stage $(T_{b,i} - T_{d,i})_j$ will tend to be larger for the cascade with fewest stages. This is because of a more rapid reduction of the driving force at the distillate downstream arising from the lower linear velocities for fewer stages with more layers, so that the area is not as well exploited. On the other hand, the fewest stages give the lowest distillate-side pressure decrease across the cascade. This exceeds 1 bar for the case of six modules in series and would probably require using intermediate pumping on the distillate side to keep the overall pressure difference between brine and distillate to a reasonable value. Finally, using more internal stages generates a smaller temperature of closest approach and thus a larger GOR. This shows that even in the case where the membrane area per cascade are equal (unlike the case in Figure 11), having more internal stages increases energy efficiency as the cascade more closely approaches true countercurrent operation.

4. Economic Optimization

4.1. Economic Estimates for DCMD with Various Heat Sources. Using the results from section 3, we can now generate

an economic optimization for the number of identical stages used to operate between a given top brine temperature $T_{b,i}$ and a limited range of brine bottom temperatures. To do this, we must parametrize the costs associated with the operation of the DCMD cascade. In particular, we must calculate those costs associated with the DCMD module, and heat exchanger cascade, and those costs associated with the energy usage.

To relate the capital costs per square meter of DCMD and HX to water production costs, we developed the following relations of specific DCMD and heat recovery HX area required ($m^2/(m^3\ h)$ of product distillate):

$$\bar{A}_{DCMD} \equiv \frac{A_{DCMD}}{\dot{m}_v}\ (m^2/(mt/h)) = \frac{\bar{a}N}{R} \tag{21}$$

where $\bar{a}$ is expressed in terms of m^2 DCMD stage/(mt/h) feed, and

$$\bar{A}_{HX} \equiv \frac{A_{HX}}{\dot{m}_V}(m^2/(mt/h)) = \frac{Q_{HX}}{\dot{m}_V U_{HX}\Delta T_{HX}} = \frac{C_P\,\dot{m}_{b,i}(T_{b,HXo} - T_{b,HXi})}{\dot{m}_V U_{HX}\Delta T_{HX}}$$
$$= \frac{C_P(\Delta T_{cascade} - \Delta T_{HX} - \Delta T_{end})}{RU_{HX}\Delta T_{HX}}$$
$$\approx \frac{\Delta H_V}{\eta_{overall}U_{HX}\Delta T_{HX}} \times \frac{(\Delta T_{cascade} - \Delta T_{HX} - \Delta T_{end})}{\Delta T_{cascade}} \tag{22}$$

For the DCMD modules and heat exchanger, we express the module costs in terms of the cost per square meter (DMC and HXC) and use an installation factor (IF) to account for related piping and installation labor and an indirect capital charge (ICC) (see Table 2 for the values of these parameters). For the DCMD module, we must also include a replacement cost (CARD) to allow for the finite lifetime of the DCMD module, as expressed by the rate of annual membrane replacement (MR). Using an annual capital charge rate (see CC in Table 2), we developed an annualized cost per square meter for membrane distillation modules (CAD) and heat exchanger area (CAH). This is given by the following:

$$CAD = DMC \times (1 + IF) \times (1 + ICC) \times CC \tag{23a}$$
$$CAH = HXC \times (1 + IF) \times (1 + ICC) \times CC \tag{23b}$$
$$CARD = DMC \times MR \tag{23c}$$

In addition, we include an annual fixed capital cost (COE) for those parts of the unit that do not scale with membrane area (electrical, instrumental, etc.). The total annualized capital costs, per m^3/d of distillate production, will then be given by the following:

$$COE = \$16.4/y/(m^3/day) \qquad \text{(from ref 13)} \tag{24a}$$
$$DCMD = \left(\frac{CAD + CARD}{24}\right) \times \left(\frac{\bar{a}N}{R}\right) \tag{24b}$$
$$HX = \left(\frac{CAH}{24}\right)\bar{A}_{HX} \tag{24c}$$
$$CAP = COE + DCMD + HX \tag{24d}$$

where DCMD and HX refer to the annualized capital costs related to membrane distillation modules and heat exchangers, respectively. The values of COE, CAD, CARD, and CAH are provided in Table 3. CAP is the total specific annual cost (expressed in terms of $\$/y/(m^3/d)$) that is due to capital and membrane replacement. It can be converted to a cost per cubic meter of distillate by dividing by the days of the year of plant operation:

$$CAP\ (\$/m^3) = \frac{CAP(\$/y/m^3/d)}{OF \times 365} \tag{25}$$

where OF is the plant online factor (see Table 2). Using these data, we can calculate capital costs as a function of the number of crossflow stages N used in the DCMD cascade (primarily, the term DCMD in eq 24b). N is related to the operating conditions through $\Delta T_{cascade}$ and ΔT_{end} (see Figure 9).

Energy costs will be obtained from the steam or steam equivalent heating costs and the pumping costs. The specific steam costs (SC, expressed in terms of $\$/m^3$ distillate) are related to heating costs CS (found in Table 3) by

$$SC(\$/m^3\ distillate) = \frac{CS}{GOR} \tag{26}$$

For example, heating costs of \$4/mt equivalent of steam would be the same as \$0.17/MJ of thermal energy.

The pumping costs (PC) are due almost entirely to the pressure decrease on the distillate side of the DCMD modules. For a specific membrane area of 2.9 m^2/(mt/h) of feed (or distillate), the distillate flow velocity is ~30 cm/s, for which the pressure drop per stage, $\Delta P_{d,stage}$ will be ~0.23 bar, allowing a pressure drop of 0.045 bar each for the entrance and exit effects. With this value, we can now calculate the pumping contribution to the energy costs, where EC is the electricity costs (found in Table 3):

$$PC = \left(\frac{N\Delta P_{d,stage}\cdot .0278(kWh/(bar\ m^3))}{\eta_{pump}R_{cascade}}\right) \times EC \tag{27}$$

The total energy costs are simply equal to SC + PC. We have assumed that the energy costs for cooling of the distillate stream prior to entering the DCMD cascade are zero, because the sea serves as an infinite cold sink. We have also neglected the cost of any pressure drop in such a heat exchanger.

Note that this is not a complete economic analysis, but only a selective one for comparing the tradeoffs between energy and

Table 2. Capital Cost Factors Used in Economic Analysis

case	conventional	large-scale, polymer HX
performance factors		
stage area/rate of feed, $\bar{a}$	2.9 m^2/(mt/h)	2.9 m^2/(mt/h)
U_{HX}	8183 kJ/(h m^2 C)	3600 kJ/(h m^2 C)
distillate pump efficiency, η_{pump}	82%	82%
heat exchange and DCMD area costs		
DMC, DCMD		
present	\$88.8/m^{2a}	
projected	\$50/m^{2a}	\$20/m^2
heat-exchanger costs, HXC	\$92.3/m^{2b}	\$20/m^2
other equipment costs	\$171.0/(mt/d)[a]	\$171.0/(mt/d)[a]
financial factors		
installation factor, IF	1.67	1.67
indirect capital costs, ICC	33%	33%
annualized capital charge rate, CC	7.2%	7.2%
DCMD replacement charge (lifetime of 7 yr), MR	14.3%	14.3%
online factor, OF	90%	90%

[a] Data taken from Sirkar and Li.[13] [b] Data taken from Peters and Timmerhaus.[14]

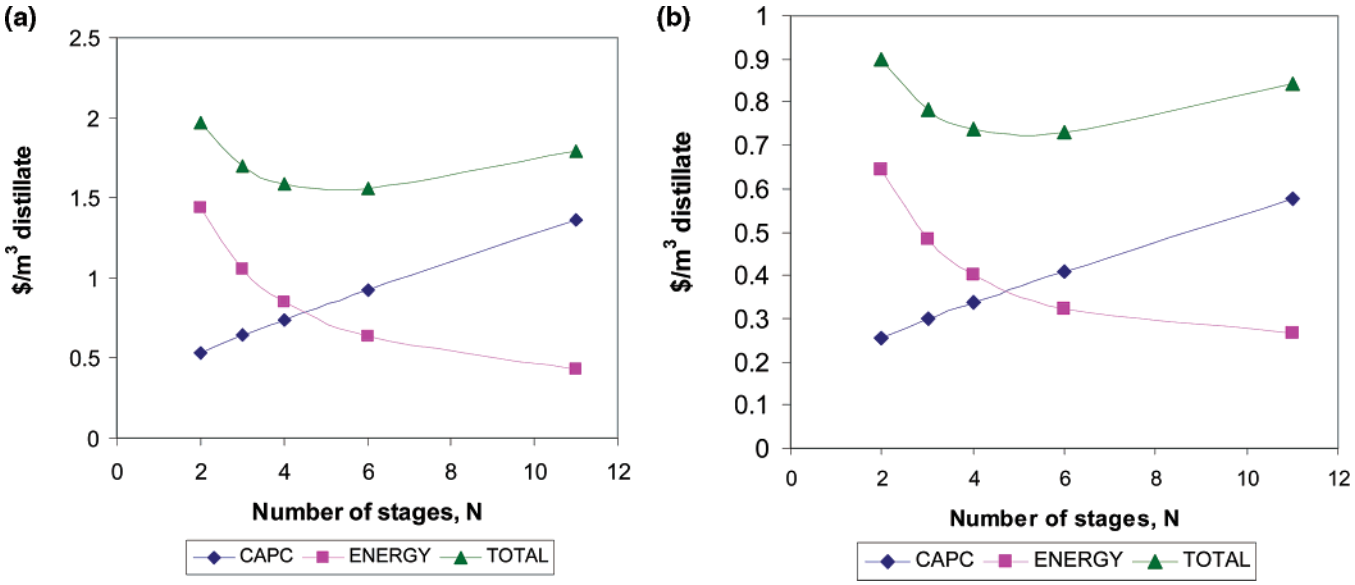

Figure 13. Optimization of costs for cascade with a top brine temperature of 95 °C and an exit brine temperature of 30−40 °C. Specific stage area is 2.9 m^2/(mt/h) of feed. Costs are as follows: (a) DCMD membrane cost of \$50/m^2, HX surface at \$92/m^2, and steam cost of \$4/mt; (b) DCMD and HX costs of \$20/m^2 and steam cost of \$1.76/mt.

Table 3. Cost Factors Used in Calculating Distillate Production Costs by Crossflow DCMD with Energy Recovery

item	conventional (present estimates)	large-scale DCMD and polymeric HX
annual CAP cost other equipment, COE	\$16.37 US/(yr m^3/d)	\$16.37 US/(yr m^3/d)
annual CAP cost (DCMD), CAD	\$8.00 US/(yr m^2)	\$2.93 US/(yr m^2)
annual CAP cost (HX), CAH	\$14.75 US/(yr m^2)	\$2.93 US/(yr m^2)
DCMD replacement, CARD	\$7.14 US/(yr m^2)	\$2.86 US/(yr m^2)
heating costs, CS	\$4.00 US/mt stream equivalent	\$0.73−4.0 US/mt stream equivalent
electricity, EC	\$0.06 US/(kW h)	\$0.06 US/(kW h)

capital related to membrane and heat exchanger area. Therefore, we did not include civil, water, and utilities capital costs, because we analyze for the case of an existing site. Also, we did not include labor, maintenance, or chemicals in the operating costs, because these will not be affected by the number of stages in a cascade.

The results for the case using conventional heat exchangers and present costs is shown in Figure 13a, assuming a steam cost of \$4/mt. It is seen that distillate costs are ∼\$1.60/m^3. Although these costs are fairly high, compared to large-scale RO, it is somewhat lower than that of conventional evaporators used for brine disposal. Note that with this relatively high steam cost, the optimum cascade has six stages in series.

If one takes a larger-scale unit with polymeric hollow tube heat exchangers for heat recovery and costs comparable to those of the RO membrane for the hollow fibers (see the last column in Table 4), then one obtains Figure 13b for the case of waste steam costing \$1.76/mt, which was toward the low value found in ref 14. If there is waste heat in the form of exhaust gases from other processes, then the energy costs may be even lower. The effect of energy costs on overall distillate production costs (expressed in terms of dollars per cubic meter of net distillate produced) is shown in Figure 14. As can be seen, as the energy costs decrease, the optimum number of crossflow stages for an individual cascade also decrease, thereby increasing flux and reducing capital costs. At \$0.73/mt steam equivalent, the distillate costs become competitive with the costs of large-scale seawater RO.

Conclusions

A methodology has been presented for incorporating crossflow DCMD modules in a countercurrent cascade, to maximize energy recovery. The methodology is based on the results from a simulator that show a linear relationship between the temperature of closest approach in the DCMD module and the decrease in brine temperature. In addition, heat balances show that the temperature of closest approach should be relatively constant for each crossflow stage in the cascade. This allows determination of the number of stages of equal-area modules needed to span the decrease in brine cascade temperature ($T_{b,i} - T_{b,o}$) in a manner similar to a McCabe−Thiele diagram. Economic optimization will involve a tradeoff between the DCMD membrane area and the heat exchanger area on one hand and energy on the other, as in other thermal processes.

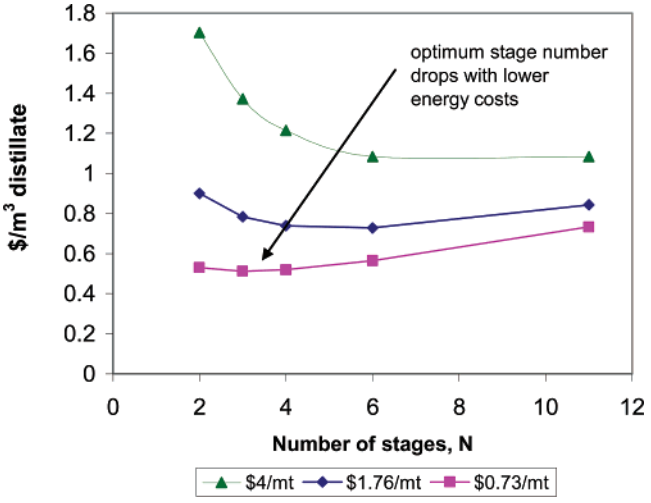

Figure 14. Impact of energy costs (\$/mt steam equivalent) on distillate costs for low-cost DCMD modules and plastic hollow-fiber heat exchangers.

Acknowledgment

This work was supported by the Office of Naval Research, through the EUWP program (Contract No. N000140510803). Part of the work was performed in the framework of author J.G.'s sabbatical from Ben Gurion University.

Notation

A_{DCMD} = DCMD membrane lumen-side area (m^2)
$\bar{A}_{DCMD}$ = specific DCMD area (m^2/(mt/h distillate production))
A_{HX} = heat exchanger area (m^2)
$\bar{A}_{HX}$ = specific heat exchanger area (m^2/(mt/h distillate production))
A_{rf} = area ratio for feed side of fiber; $A_{rf} = d_o/d_i$
A_{rp} = area ratio for permeate side of fiber; $A_{rp} = d_o/d_i$
A_{rln} = logarithmic membrane area ratio for fiber; $A_{rln} = d_{lm}/d_i$
$\bar{a}$ = specific stage area, m^2 of one stage in cascade per (mt/h of feed)
CAD = annualized cost per m^2 for DCMD, eq 23 ($/(yr m^2))
CAH = annualized cost per m^2 for heat exchanger, eq 23 ($/(yr m^2))
CAP = total specific annual cost, eq 24, $/(yr m^3/d))
CARD = annualized cost for DCMD membrane replacement ($/(yr m^2))
CC = annual capital charge rate (%)
COE = specific annual fixed capital cost, from eq 24 ($/(yr m^3/d))
CS = steam cost ($/mt)
C_P = heat capacity (kJ/(kg °C))
DCMD = specific annual costs directly related to the DCMD membrane module, from eq 24 ($/(yr m^3/d)); direct contact membrane distillation
D_i = diffusion coefficient of species *i*
d_i = hollow fiber inner diameter (m)
d_{lm} = logarithmic mean diameter of hollow fiber; $d_{lm} = (d_o - d_i)/\ln(d_o/d_i)$ (m)
d_o = hollow fiber outside diameter (m)
GOR = gained output ratio, expressed in terms of mt distillate produced per mt steam equivalent
H = specific enthalpy (kJ/kg)
ΔH_V = heat of vaporization (kJ/kg)
h_f = film heat-transfer coefficient for brine side, from eq 9 (kJ/(h m^2 °C))
h_m = membrane heat-transfer coefficient, from eq 10 (kJ/(h m^2 °C))
h_p = film heat-transfer coefficient for distillate side, from eq 9 (kJ/(h m^2 °C))
h_{mg} = heat-transfer coefficient of the gas phase in the porous membrane, equation (kJ/(h m^2 °C))
h_{ms} = heat-transfer coefficient of the solid phase in the porous membrane (kJ/(h m^2 °C))
HX = specific annual costs directly related to heat recovery heat-exchanger area, eq 24 ($/(yr m^3/d))
HXC = heat-exchanger costs ($/$m^2$)
IF = installation factor, defined as the ratio of installed to purchase cost
ICC = indirect capital charge
k_m = effective water vapor permeance (kg/(m^2 h Pa))
L = length of a hollow fiber (m)
MR = rate of annual membrane replacement (%)
$\dot{m}_{b,i}$ = brine flow rate into DCMD unit (kg/h)
$\dot{m}_{b,o}$ = brine flow rate out of DCMD unit (kg/h)
$\dot{m}_{d,i}$ = distillate flow rate into DCMD unit (kg/h)
$\dot{m}_{d,o}$ = distillate flow rate out of DCMD unit (kg/h)
$\dot{m}_f$ = fresh feed flow rate (kg/h)
$\dot{m}_{rej}$ = rejected brine flow rate (kg/h)
$\dot{m}_V$ = distillate production rate (kg/h)
n_j = number of fibers in the *j*th layer
N = number of XF-DCMD stages in a cascade
N_v = water vapor flux based on log mean area; see eq 11 (kg/(m^2 h))
PC = specific pumping costs ($/$m^3$)
P_{fm} = partial pressure of water vapor of brine-membrane interface (Pa)
P_{pm} = partial pressure of water vapor of distillate−membrane interface, (Pa)
Q_{in} = brine heat input; see eq 2 (kJ/h)
$Q(x)$ = rate of heat transfer across the membrane from the distillate entrance up to a point x along fiber axis in a particular fiber layer, eq 15 (kJ/h)
$\Delta P_{d,stage}$ = distillate side pressure drop per stage (bar)
R = fractional water recovery, from eq 3
SC = specific steam cost ($/$m^3$ distillate)
T(x) = local temperature at point *x* along the fiber axis (°C)
$T_{b,HX,i}$ = brine temperature entering the heat recovery heat exchanger (°C)
$T_{b,HX,o}$ = brine temperature exiting from the heat recovery heat exchanger (°C)
$T_{b,i}$ = brine inlet temperature to DCMD (°C)
$T_{b,o}$ = brine outlet temperature from DCMD (°C)
$T_{d,HX,i}$ = distillate temperature entering the heat recovery heat exchanger (°C)
$T_{d,HX,o}$ = distillate temperature exiting from the heat recovery heat exchanger (°C)
$T_{d,i}$ = distillate inlet temperature to DCMD (°C)
$T_{d,o}$ = distillate outlet temperature from DCMD (°C)
T_f = temperature of fresh feed (°C)
ΔT_{HX1} = temperature differences between hot and cold streams at the distillate stream exit of heat exchanger 1; from Figure 2 (°C)
ΔT_{HX2} = temperature differences between hot and cold streams at the distillate stream exit of heat exchanger 2; from Figure 2 (°C)
$\Delta T_{end} = T_{b,i} - T_{d,o}$ (°C)
$\Delta T_{stage} = T_{b,i} - T_{b,o}$ (°C)
$\langle T_{b,m} \rangle$ = average brine temperature at the membrane surface weighted by vapor flux at each temperature (°C)
U_{HX} = overall heat-transfer coefficient for heat exchanger (kJ/(h m^2 °C))

Greek Symbols

α = lumen-side surface area per unit length in the *j*th layer of the XF-DCMD module; $\alpha = n_j \pi d_i$ (m)
η = thermal efficiency; fraction of total enthalpy transferred from brine to distillate that is transferred by vapor
ρ = density (kg/m^3)

Subscripts Used with T(x)

f = brine side of fiber
p = distillate side of fiber
m = membrane surface
j = *j*th layer in a multilayer DCMD module, or *j*th module in a multimodule cascade or stage

Subscripts

DCMD = direct contact distillation module
HX = heat-exchanger module

Literature Cited

(1) Lawson, K. W.; Lloyd, D. R. Membrane distillation−Review. *J. Membr. Sci.* **1997**, *125*, 1.

(2) Alkali, A. M.; Lior, N. Membrane−Distillation desalination: Status and potential. *Desalination* **2004**, *171*, 111.

(3) Curcio, E.; Drioli, E. Membrane Distillation and Related Operations−A review. *Sep. Purif. Rev.* **2005**, *34*, 35−86.

(4) Fane, A. G.; Schofield, R. W.; Fell, C. J. D. The efficient use of energy in membrane distillation. *Desalination* **1987**, *64*, 231.

(5) Koschikowski, J.; Wieghaus, M.; Rommel, M. Solar thermal-driven desalination plants based on membrane distillation. *Desalination* **2003**, *156*, 295−304.

(6) Li, B.; Sirkar, K. K. Novel membrane and device for direct contact membrane distillation-based desalination process. *Ind. Eng. Chem. Res.* **2004**, *43*, 5300−5309.

(7) Song, L.; Li, B.; Sirkar, K. K.; Gilron, J. L. Direct contact membrane distillation-based desalination: Novel membranes, devices, larger-scale studies and a model. *Ind. Eng. Chem. Res.* **2007**, *46*, 2307.

(8) Kreith, F.; Bohn, M. S. *Principles of Heat Transfer*, Sixth Edition; Brooks/Cole, Pacific Grove, CA; pp A14−A15 (Table 13, water at saturation pressure).

(9) Gryta, M.; Tomaszewska, M. Heat Transport in the membrane distillation process. *J. Membr. Sci.* **1998**, *144*, 211.

(10) Žukauskas, A. Heat transfer from tubes in crossflow. In *Advances in Heat Transfer*, Vol. 8; Hartnett, J. P., Irvine, T. F., Jr., Eds.; Academic Press: New York, 1972; p 93.

(11) Li, B.; Sirkar, K. K. Novel membrane and device for vacuum membrane distillation-based desalination process. *J. Membr. Sci.* **2005**, *257*, 60.

(12) Zarkadas, D. M.; Sirkar, K. K. Polymeric hollow fiber heat exchangers: An alternative for lower temperature applications. *Ind. Eng. Chem. Res.* **2004**, *43*, 8093.

(13) Sirkar, K. K.; Li, B. Novel membrane and device for direct contact membrane distillation-based desalination process: Phase III. Desalination and Water Purification Research and Development Program Final Report No. 99, U.S. Bureau of Reclamation, Denver, CO, May 18, 2005.

(14) Peters, M. S.; Timmerhaus, K. D. *Plant Design and Economics for Chemical Engineers*, 4th Edition; McGraw−Hill: New York, 1991; p 815 (Table 5).

Received for review July 30, 2006
Revised manuscript received January 18, 2007
Accepted January 21, 2007

IE060999K